ACS OMEGA

Open Access

http://pubs.acs.org/journal/acsodf

Article

Two Novel Metformin Carboxylate Salts and the Accidental Discovery of Two 1,3,5-Triazine Antihyperglycemic Agent

Qi An,[#] Na Li,[#] Zhehui Zhao, Nuoqi Wang, Xueying Wang, Xiuying Yang, Dezhi Yang,* Li Zhang,* Yang Lu,* Guanhua Du, and H. C. Stephen Chan*

Cite This: *ACS Omega* 2023, 8, 48028−48041

Read Online

ACCESS | Metrics & More | Article Recommendations | Supporting Information

ABSTRACT: Metformin (MET), commonly marketed as a hydrochloride salt (MET-HCl) for better pharmacokinetic profile over the free base, would release a high concentration of chloride ions and cause adverse gastrointestinal effects. The preparation of chloride-free MET salts could potentially circumvent this issue. In this study, seven carboxylic acids (formic acid, acetic acid, malonic acid, succinic acid, fumaric acid, cinnamic acid, and acetylsalicylic acid) were used for preparing MET carboxylate salts. When compared with MET-HCl, all MET salts/salt hydrates show lower dissolution rates in pH 6.8 phosphate buffer. However, the cinnamic acid and acetylsalicylic acid show significantly higher dissolution rates in the forms of MET salt/salt hydrate. In the permeability test, the permeability of the MET in all of the salts was not improved. However, the permeability of cinnamic acid in the MET cinnamate is reduced, and the permeability of acetylsalicylic acid in the MET acetylsalicylate is increased. Meanwhile, at a higher crystallization temperature, the acetone solvent and a hydrolyzed product of acetylsalicylic acid react with MET respectively, leading to two unexpected 1,3,5-triazine derivatives. The results of *in vitro* bioactivity assays indicate that one of the triazine molecules promote glucose consumption more effectively than MET-HCl, and had relatively weak lactate production ability at low concentration. This glucose metabolism regulating compound may serve as a novel lead antihyperglycemic agent for further optimization.

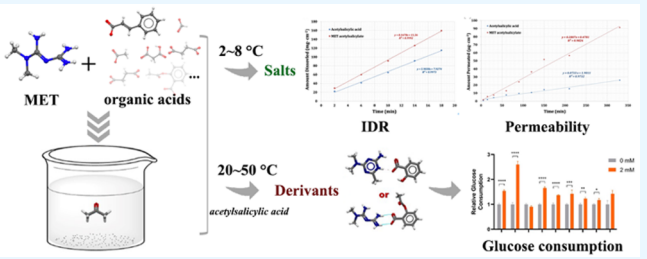

1. INTRODUCTION

As a first-line agent against non-insulin-dependent diabetes mellitus,[1] metformin (MET) has been shown effective in improving insulin resistance and reducing blood glucose and lipids.[2] Its anti-inflammation and antiaging properties have also been reported.[3] MET suppresses hyperglycemia by inhibiting hepatic gluconeogenesis, activating adenosine 5′-monophosphate (AMP)-activated protein kinase, and regulating mitochondrial functions. Currently, most MET products are marketed as hydrochloride salt form (MET-HCl), of which the intestinal absorption is over two times better than MET free base.[4−6] Despite its widespread use in clinical practice, patients after prolonged use of MET-HCl are prone to develop gastrointestinal disorders, due to the release of high concentration of chloride ions.[5,7,8] Hence, replacing the chloride ion with other possible counterions would be a viable option in resolving the adverse effect of the existing MET solid form. In this study, seven carboxylic acids, namely, formic acid, acetic acid, malonic acid, succinic acid, fumaric acid, cinnamic acid, and acetylsalicylic acid, were chosen for preparing MET salt forms. Except for fumarate hydrate and cinnamate hydrate, the crystal structures of other MET salts have been reported.[9−13] However, not all the reported crystal forms were thoroughly investigated for their physicochemical properties relevant to pharmaceutical profile. For example, MET acetate was reported for its antimicrobial activity, without any data of its intrinsic dissolution rate and aqueous solubility. Moreover, cinnamic acid and acetylsalicylic acid are pharmaceutically active.[14,15] The formation of MET salt with these molecules may achieve combinatory or even synergistic therapeutic effects.

All seven MET-carboxylate salt crystals obtained in this study were then subject to a series of solid-state characterization experiments, X-ray structure analysis, and theoretical calculation. Solubilities in pH 6.8 phosphate buffer were measured by the equilibrium solubility and intrinsic dissolution rate (IDR) test. Among these, the measurement of the IDR is regarded as one of the most important indicators for developing a new chemical entity. IDR may be used for predicting potential bioavailability problems and for characterizing compendial articles, such as excipients or drug

Received: September 5, 2023
Revised: November 12, 2023
Accepted: November 15, 2023
Published: December 8, 2023

Scheme 1. Three Crystallized Products from a Mixture of MET and Acetylsalicylic Acid under Different Experimental Conditions

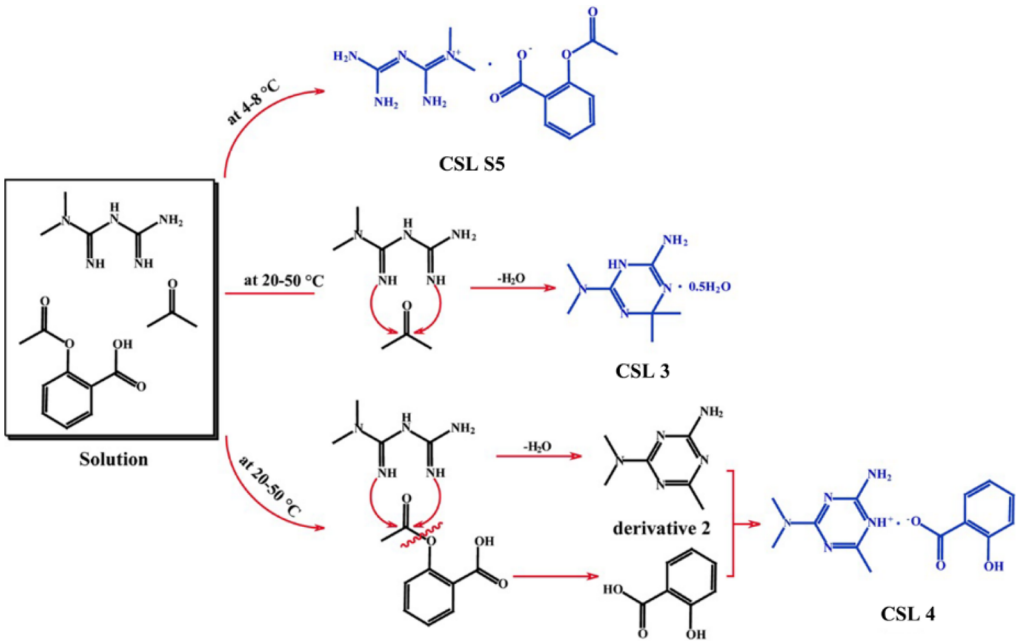

substances.[16] Simultaneously, the permeability experiment was also carried out using the Franz diffusion cell method to evaluate the permeability changes in metformin or the corresponding ligand.[17] Besides characterizing their physicochemical properties, *in vitro* bioassays were also performed to investigate whether these carboxylate salts would possess better antihyperglycemic activities and cytotoxicity profiles, when compared to MET-HCl.

Noticeably, an interesting event occurred during the preparation of the MET acetylsalicylate salt in acetone. Two unexpected crystalline products emerged under different crystallization conditions. Fourier transform infrared (FTIR) results hint that the chemical compositions in these solid forms may have been altered. Single crystal X-ray Diffraction (SXRD) confirms two different 1,3,5-triazine compounds crystallized as a hemihydrate and a salicylate salt, respectively. The two triazines are almost identical except that the former has one additional methyl group. From this subtle structural difference, one may speculate that the former triazine is likely a reaction product between MET and acetone, whereas the latter triazine could be formed after MET reacts with the acetyl group of acetylsalicylic acid. Despite the diverse biological activities from triazine compounds, the intriguing question is whether the two unexpected triazines in our study would possess antihyperglycemic activity similar to MET-HCl. Encouragingly, the triazine hemihydrate at low dose (2 mM) shows an excellent promotion of glucose consumption in HepG2 cells with tolerable cytotoxicity and appears to be a promising candidate for further lead optimization. However, its structural analogue from the salicylate salt shows no similar bioactivity at all. Why two highly similar analogs exhibit distinctly different biological activities remains an open question for future research.

2. MATERIALS AND METHODS

2.1. Materials. MET-HCl and acetylsalicylic acid were purchased from Jiuding Chemistry Biotechnology Co., Ltd. Formic acid, acetic acid, malonic acid, fumaric acid, and succinic acid were purchased from Sinopharm Chemical Reagent Beijing Co., Ltd., whereas cinnamic acid was purchased from Wuhan Far Cheng Co. Creation Technology Co., Ltd. Analytical grade acetone used for crystallization and sodium hydroxide were purchased from Beijing Chemical Works. HepG2 cells (C5 passage, human hepatoma cell line) were purchased from the National Platform of Experimental Cell Resources for Sci-Tech, Chinese Academy of Medical Sciences (Beijing, China).

2.2. Syntheses of Metformin Carboxylate Salts and 1,3,5-Triazine Derivatives. About 1 mmol of MET-HCl and sodium hydroxide were first dissolved in 50 mL of acetone with constant stirring for about 4 h. Next, formic acid, acetic acid, malonic acid, succinic acid, fumaric acid, cinnamic acid, or acetylsalicylic acid was slowly added, respectively, until the solution pH was adjusted to 6−7. After stirring for another 4 h, the solution was then filtrated and left still at 4−8 °C for crystal growth. Finally, colorless, transparent crystals were harvested from the solution. The crystal of fumaric acid and cinnamic acid was labeled as CSL 1 and 2, respectively, and the crystal of formic acid, acetic acid, malonic acid, succinic acid, and acetylsalicylic acid was labeled as CSL S1−5. Notably, when the temperature for crystal growth was set between 20−50 °C for a mixture containing 1 mmol acetylsalicylic acid, two different 1,3,5-triazine compounds were formed (Scheme 1): (a) MET reacted with acetone and a new triazine molecule crystallized as a hemihydrate (CSL 3); (b) MET reacted with acetylsalicylic acid and resulted in a 1:1 salt of another triazine (namely, derivative 2) and the salicylate ion (CSL 4). Both CSL 3 and CSL 4 are colorless and transparent.

2.3. Spectroscopic Analysis. *2.3.1. Powder X-ray Diffraction (PXRD).* PXRD patterns were measured using a Rigaku SmartLab 9KW diffractometer with Cu K_α radiation (Rigaku, Tokyo, Japan). Finely pulverized samples with an agate mortar were subjected to X-ray radiation and measured

https://doi.org/10.1021/acsomega.3c06721
ACS Omega 2023, 8, 48028−48041

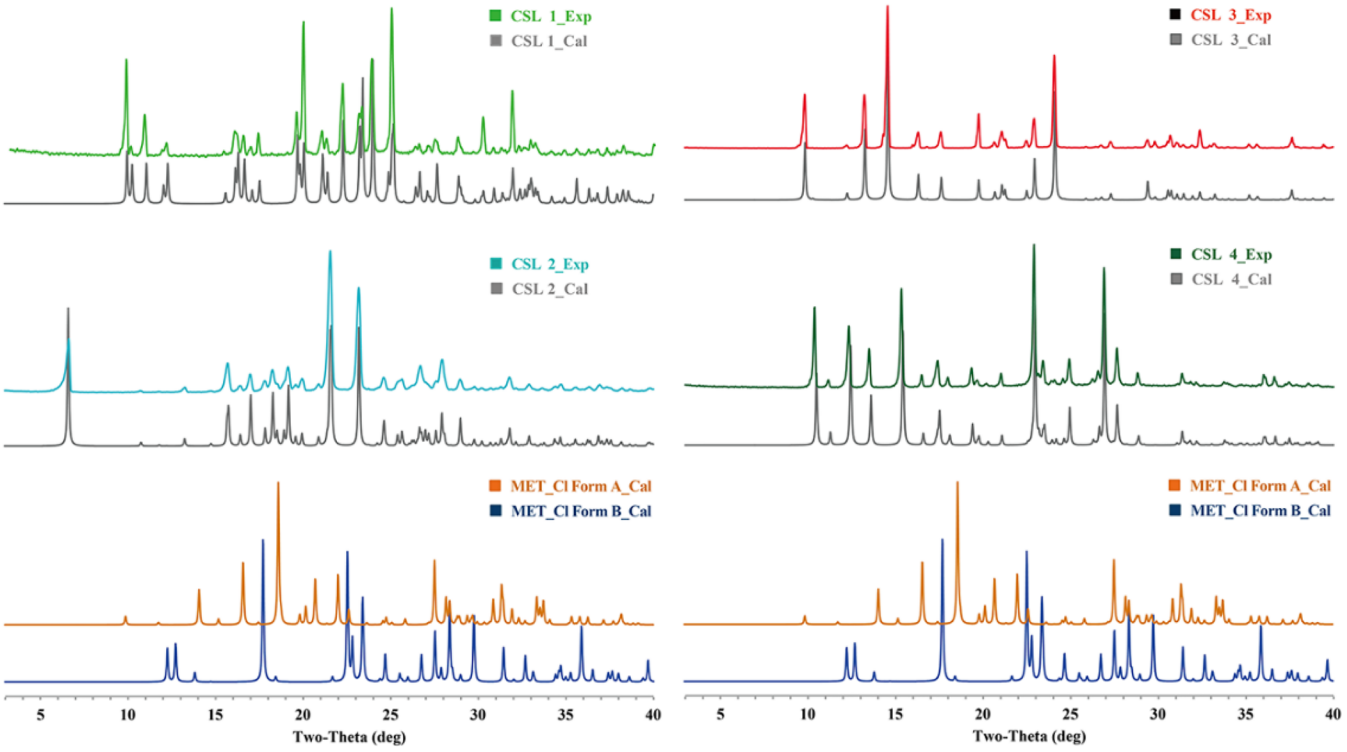

Figure 1. Experimental PXRD patterns of MET organic acid salt (Exp) and their simulated patterns (Cal) alongside those of MET-HCl forms A and B.

at 2θ range of 3−40° at a constant rate of 8°/min. Data were further processed using JADE software (Rigaku). Simulated PXRD patterns were calculated from the experimental cif files using CCDC Mercury software Version 2023.1 within the same 2θ range,[18] where a full width at half-maximum (fwhm) of 0.15° and a default step size of 0.02° were used.

2.3.2. Fourier Transform Infrared (FT-IR) Spectroscopy. Samples were analyzed using a PerkinElmer Spectrum 400 FT-IR spectrophotometer (PerkinElmer, Massachusetts) with an attenuated total reflectance (ATR) sampling accessory. The scanning range was set between 650 and 4000 cm^{-1} with 4 cm^{-1} resolution. The collected spectra were further processed by using the Spectrum software suite (PerkinElmer, U.S.).

2.3.3. Single-Crystal X-ray Diffraction (SXRD). Samples were analyzed on a Rigaku MicroMax-002$^+$ CCD diffractometer with Cu−Kα radiation (λ = 1.54178 Å) (Rigaku, Americas, the Woodlands, Texas). Absorption correction and integration of the collected data were handled using the CrystalClear software package (Rigaku Americas). The crystal structures were resolved using the Olex^2 crystallography software platform.[19] Structure determination was achieved by direct method, followed by Fourier synthesis with SIR2008.[20] The refinement on F^2 was performed via the full-matrix least-squares procedures in SHELXL.[21] For non-hydrogen atoms, anisotropic displacement parameters (ADPs) were introduced, whereas hydrogen atoms were refined isotropically with an isotropic atomic displacement parameter (U_{iso}) that is 1.2 times the value of the parent atom. Those from the methyl or hydroxyl groups were assigned 1.5 times that of the parent atom. The hydrogen atoms were placed in ideal positions and refined using the riding model, whereas hydrogen atoms involved in the hydrogen bonding were detected in the experimental electron density map and refined freely. Refinement of disorders with restraints was introduced to help data convergence.[22]

2.4. Intrinsic Dissolution Rate (IDR). MET-HCl, MET carboxylate salts CSL 1 and 2, and CSL S1−5 were measured for their IDRs. Samples containing 300.0 mg of MET (in equivalence) were compacted into round discs of 8 mm diameter, using a flat-faced round punch (FU KESI, China). Static disc method was performed at 75 rpm in 900 mL of pH 6.8 phosphate buffer at 37 ± 0.5 °C for 18 min. The detection time points were set at 2, 6, 10, 14, and 18 min. In addition, an IDR test was also performed at 300 rpm in 700 mL of 90% isopropyl alcohol−water solution at 37 ± 0.5 °C for 60 min to investigate the dissolution rate of the organic solvent system. MET concentration in the solution was measured using a HPLC method for MET-HCl in Chinese Pharmacopoeia.[23] Chromatographic conditions are as follows: the chromatographic column was Welch Ultimate XB-SCX (4.6 × 250 mm, 5 μm), the mobile phase was 1.7% $NH_4H_2PO_4$ solution (adjust the pH to 3.0 with phosphoric acid), the detection wavelength was 218 nm and the injection volume was 10 μL.

2.5. Equilibrium Solubility. In order to compare the water solubility of these salts, the equilibrium solubilities of these salts in pH 6.8 phosphate buffer. The excess sample was added to 5 mL buffer medium, stirred at 37 ± 0.5 °C for 72 h, and then filtered through a membrane filter after 24 h of equilibration. Take 0.5 mL of filtrate into a 250 mL volumetric flask, add pH 6.8 phosphate buffer to volume to the scale mark, and shake well. The content of metformin was measured HPLC method as described in section 2.4.

2.6. Permeability Analysis. Permeability experiments of MET cinnamate and MET acetylsalicylate were measured by the vertical Franz diffusion cell apparatus through the cellulose nitrate membrane (cytiva Whatman, 0.45 μm,

https://doi.org/10.1021/acsomega.3c06721
ACS Omega 2023, 8, 48028−48041

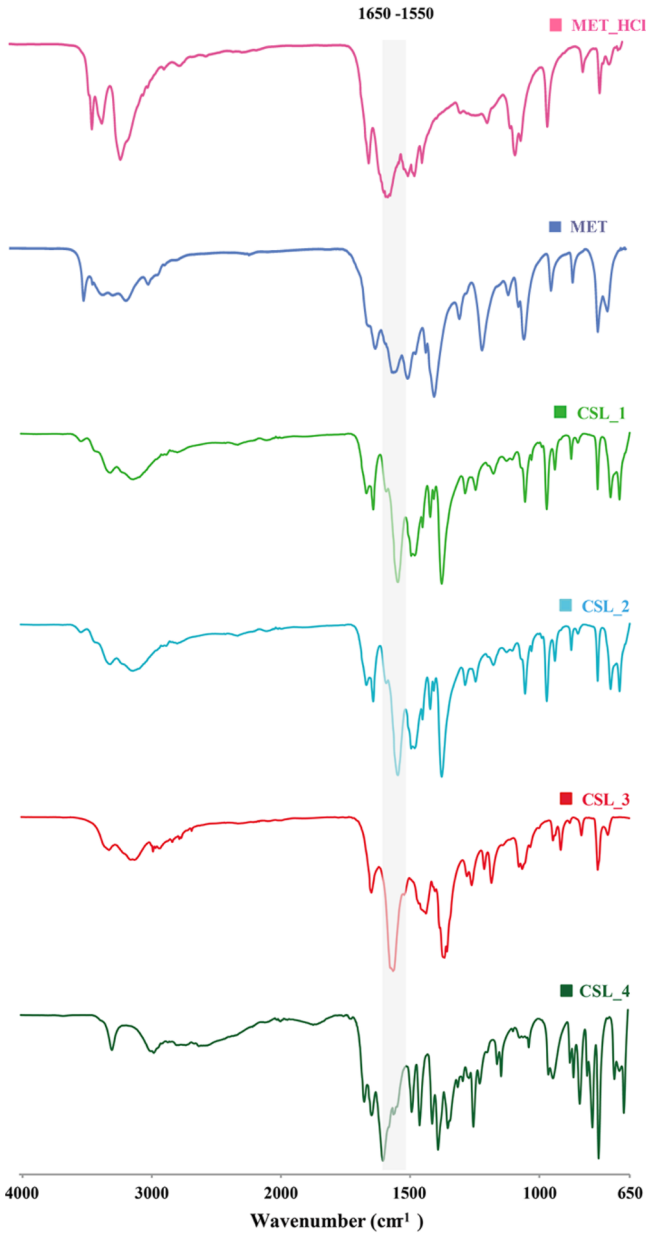

Figure 2. FT-IR spectra of CSL 1−4. The IR band within the highlighted region of 1550 to 1650 cm^{-1} may correspond to an asymmetric carbonyl stretch of carboxylate.

diameter 25 mm). The membrane was placed between the donor compartment and the recipient compartment, and about 8 mL of buffer medium (pH 6.8) was added. After the buffer medium was kept at 37 ± 0.5 °C, the mixture was rotated at 100 rpm. About 20 mg/mL solutions of different MET salts were placed in the donor compartment. The sample solution (0.5 mL) was extracted from the receptor chamber at the set time points and replaced with the same volume of the buffer medium. Finally, the concentrations of MET were measured by HPLC method as described in section 2.4. In addition, the concentrations of cinnamic acid and acetylsalicylic acid were simultaneously measured by the HPLC method. The chromatographic conditions are as follows: the chromatographic column was Welch Ultimate XB C18 (4.6 × 250 mm, 5 μm), the mobile phase was acetonitrile: 0.5% acetic acid aqueous solution (32:68), the detection wavelength was 278 nm and the injection volume was 10 μL.

2.7. Thermal Analysis. Differential scanning calorimetry (DSC) was performed on a DSC 1 (Mettler Toledo, Switzerland) with STARe Evaluation software 13.0. Approximately 5−8 mg were weighed into aluminum crucible and heated at 10 °C/min over the temperature range of 30−280 °C (for CSL 1 and 2, and S1−5) or 30−230 °C (for CSL 3 and 4) under a nitrogen flux of 150 mL/min. Thermogravimetric analysis (TGA) was conducted on a DSC/TGA 1 analyzer (Mettler Toledo, Switzerland) to investigate the stoichiometry of water in CSL1−3. Approximately 10 mg of the sample was added to an aluminum crucible and heated at a constant rate of 5 °C/min over the temperature range of 30 to 500 °C under a nitrogen flux of 50 mL/min.

2.8. Theoretical Calculation. *2.8.1. Packing Comparison.* Similarities in the molecular packing were evaluated with CrystalCMP software in terms of distance displacement and angle displacement of molecules in the molecular cluster.[24] A smaller deviation value indicates a higher packing similarity between two structures.

2.8.2. Conformation Analysis. Rigid grid scan was performed on the backbone dihedral angle C−N−C−$N(Me_2)$ of the MET. The initial geometry was extracted from an experimental structure. Molclus 1.9.3 was utilized to generate new conformers by altering the target dihedral angle iteratively with an increment of 5°.[25] For each conformer, single point DFT energy was calculated using M06-2X functional and TZVP basis set in Gaussian 16 package.[26]

2.8.3. Lattice Energy Calculation. The lattice energy of each experimental structure was minimized to a local energy minimum, by optimizing its structural and molecular geometries with Quantum Espresso version 6.4.[27,28] Density Functional Theory with dispersion correction (DFT-D) calculations were performed using the Perdew−Burke−Ernzerhof (PBE) functional with the projector augmented wave (PAW) pseudopotential.[29,30] The dispersion energy was corrected using the exchange-hole dipole model (XDM).[31] The kinetic energy cutoff was set to 55 Ry. The k-point distance was approximately 0.07 $Å^{-1}$. Convergence threshold on total energy was set to 1×10^{-6} Ry per atoms in the unit cell. For evaluating the internal energies of each molecular component in gas phase, Martyna−Tuckerman correction was applied to mimic an isolated environment in vacuum.[32] For the succinate anion, Gaussian smearing of 0.01 Ry was used to assist self-consistency field convergence for Brillouin-zone integration.

2.8.4. Solvation Enthalpy Calculation. Solvent effect on each isolated molecular component was treated with the conduct-like polarizable model (CPCM) implemented in software ORCA version 5.0.[33−35] The single point energy of the molecular component was calculated at the PBE/6-31G* level. The universal solvation model (SMD) was chosen to compute the cavity-dispersion energy, using the full electron density of the solute. 2-propanol was taken as the solvent medium.[36]

2.9. Glucose Consumption and Cell Viability Assays. HepG2 cells were cultured at 37 °C with 5% CO_2 and the glucose-rich (25 mmol/L) Dulbecco's Modified Eagle's Medium (DMEM), supplemented with 10% Fetal Bovine Serum (FBS). The medium was changed every 2 days.[37] Glucose consumption was assessed as described previously.[38] HepG2 cells were placed in 96-well plates and treated with

https://doi.org/10.1021/acsomega.3c06721
ACS Omega 2023, 8, 48028−48041

Table 1. Crystal Parameters, Data Collected, and Refinement Details of All MET Carboxylate Salts (CSL 1 and 2) and the Two 1,3,5-Triazine Molecules (CSL 3 and 4)

parameters	CSL 1	CSL 2	CSL 3	CSL 4
compound name	MET fumarate hydrate	MET cinnamate hydrate	MET derivative 1	MET derivative 2
empirical formula	$C_4H_{13}N_5{\cdot}C_4H_6O_4{\cdot}2H_2O$	$C_9H_7O_2{\cdot}C_4H_{12}N_5{\cdot}H_2O$	$C_7H_{15}N_5{\cdot}0.5H_2O$	$C_6H_{12}N_5{\cdot}C_7H_5O_3$
formula weight	281.28	295.35	180.26	291.32
temperature (K)	273(2)	273(2)	293(2)	293(2)
Crystal system	triclinic	monoclinic	orthorhombic	monoclinic
space group	$P\bar{1}$	$P2_1/c$	$P\bar{4}n2$	$P2_1/n$
a (Å)	8.7135(2)	14.0355(2)	12.1385(5)	8.5066(5)
b (Å)	9.3413(2)	10.4076(1)	12.1385(3)	16.8503(7)
c (Å)	9.5100(2)	11.3474(2)	13.3395(9)	11.0570(6)
α (deg)	102.020(2)	90	90	90
β (deg)	103.609(2)	108.286(2)	90	112.234(7)
γ (deg)	105.841(2)	90	90	90
Z	2	4	8	4
volume (Å^3)	692.35(3)	1573.88(4)	1965.48(16)	1467.05(15)
calc density (g·cm^{-3})	1.349	1.246	1.218	1.319
goodness-of-fit on F^2	1.062	1.088	1.099	1.025
final R, $wR(F^2)$ values $[I > 2\sigma(I)]$	0.0486, 0.1342	0.0555, 0.1632	0.0333, 0.0925	0.0467, 0.1492
CCDC deposition no.	2285965	2044985	2044987	2044986

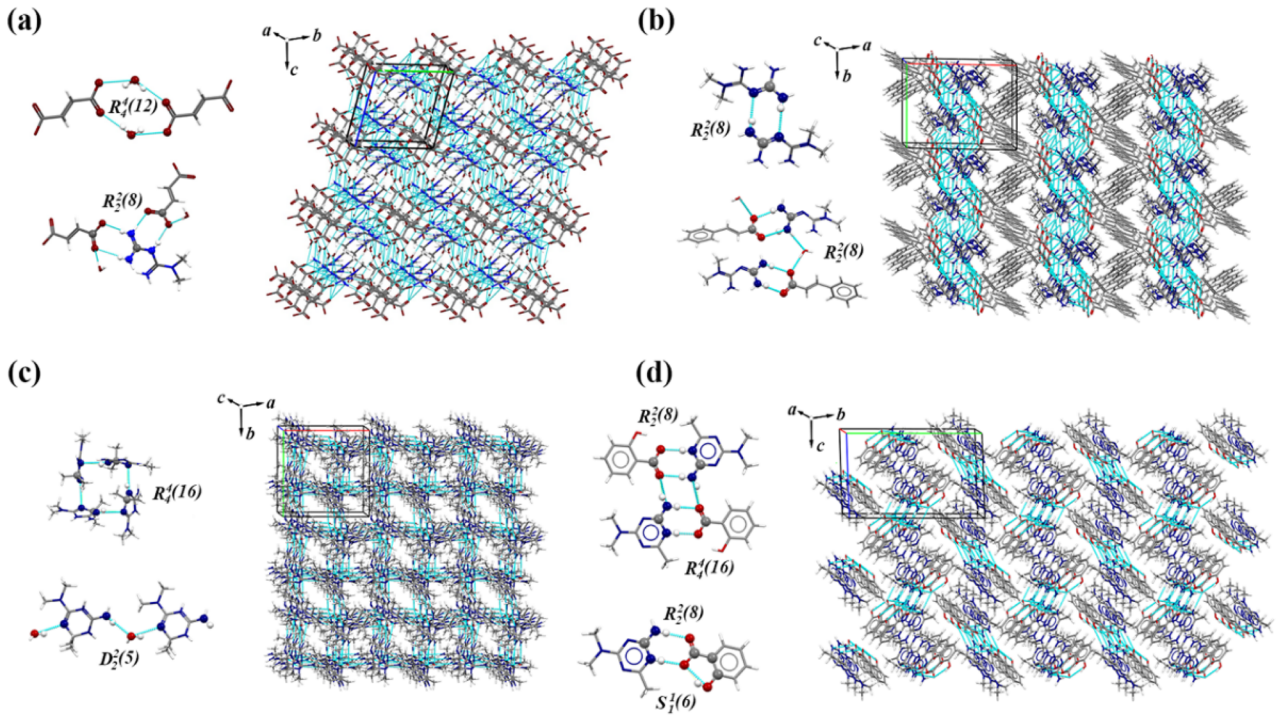

Figure 3. Important hydrogen bond motifs among the prepared MET salts: (a) fumarate dihydrate, (b) cinnamate monohydrate, (c) derivative 1, and (d) derivative 2.

different concentrations of the compounds at 37 °C and 5% CO_2. After the indicated duration, the supernatant was tested for glucose content, using a blood glucose kit from Biosino Biotechnology (Beijing, China). The amount of consumed glucose was calculated from the difference in glucose concentration between the blank well and any other test well. To evaluate the cell viability after exposure to a test compound, HepG2 cells were preincubated overnight on a 96-well plate in a cell incubator. After the treated with a test compound for a certain period of time, the reagent solutions from cell counting kit-8 (CCK-8) (Dojindo, Kumamoto, Japan) making up one-tenth of the final volume was added. The plate was further incubated in the incubator for 2 h, and the absorbance at 450 nm recorded by SpectraMax M5 microplate reader (Molecular devices, LLC. USA) reflected the amount of viable cell. The statistical difference between any two groups was tested using one-way ANOVA with Tukey posthoc analysis. Data were analyzed using GraphPad Prism (GraphPad Software, USA). Data are presented as means ± SEM. The significance level was set at $P \leq 0.05$.

3. RESULTS AND DISCUSSION

3.1. Spectroscopic Analysis. *3.1.1. PXRD.* The measured diffraction patterns of all nine crystalline products match the

https://doi.org/10.1021/acsomega.3c06721
ACS Omega 2023, 8, 48028−48041

Table 2. Hydrogen Bond Parameters (Å, degree) in MET Carboxylate Salts and the New 1,3,5-Triazine Derivatives

Compounds	D−H···A	D···A	D−H···A	D···A	D−H···A	D···A
CSL 1	$O_{2W}-H_{2WB}...O_{4A}$ [a]	2.765(10)	$O_{2W}-H_{2WB}...O_{4A}$ [b]	3.004(9)	$O_{1W}-H_{1WA}...O_1$ [c]	2.797(2)
	$N_4-H_{4B}...O_2$ [d]	2.781(2)	$N_6-H_{6A}...O_{3A}$ [e]	2.980(2)	$N_7-H_{7A}...O_{4A}$ [f]	2.980(2)
CSL 2	$N_3-H_{3A}...O_2$ [g]	2.924(6)	$N_3-H_{3B}...N_4$ [h]	3.071(7)	$N_5-H_{5A}...O_1$ [i]	2.986(7)
	$N_5-H_{5B}...O_2$	3.121(7)	$N_8-H_{8A}...O_1$ [j]	2.903(7)	$N_8-H_{8B}...O_{0AA}$ [k]	2.959(8)
CSL 3	$O_{1W}-H_{1W}...N_1$ [l]	2.907(2)	$N_2-H_2...N_1$ [m]	3.182(2)	$N_3-H_3...N_5$ [n]	3.113(2)
	$N_5-H_{5B}...O_{1W}$ [o]	2.975(2)	—	—	—	—
CSL 4	$N_1-H_1...O_2$	2.734(2)	$O_6-H_6...O_2$	2.552(2)	$N_{10}-H_{10A}...O_4$ [p]	2.842(2)

[a]Symmetry code: $-x, 2-y, 1-z$. [b]Symmetry code: $-x, 2-y, 1-z$. [c]Symmetry code: $1-x, 1-y, 1-z$. [d]Symmetry code: $1-x, 1-y, -z$. [e]Symmetry code: $1+x, y, z$. [f]Symmetry code: $1+x, y, z$. [g]Symmetry code: $x, 1/2-y, -1/2+z$. [h]Symmetry code: $1-x, -y, 2-z$. [i]Symmetry code: $1-x, 1/2+y, 5/2-z$. [j]Symmetry code: $x, 1/2-y, -1/2+z$. [k]Symmetry code: $1-x, 1-y, 2-z$. [l]Symmetry code: $1/2-y, 1/2-x, 1/2-z$. [m]Symmetry code: $1-y, x, 1-z$. [n]Symmetry code: $1/2-y, 1/2-x, 3/2-z$. [o]Symmetry code: $1-y, x, 1-z$. [p]Symmetry code: $1-x, -y, 1-z$.

Table 3. Equilibrium Solubility of MET Salts in pH 6.8 Phosphate Buffer at 37 °C

crystal	salts	equilibrium solubility (mg/mL)
—	MET hydrochloride	345.8 ± 8.4
CSL 1	MET fumarate dihydrate	112.8 ± 7.2
CSL 2	MET cinnamate monohydrate	296.6 ± 6.0
CSL S1	MET formate	279.0 ± 8.9
CSL S2	MET acetate	184.1 ± 7.3
CSL S3	MET malonate	184.7 ± 5.5
CSL S4	MET succinate monohydrate	125.6 ± 4.7
CSL S5	MET acetylsalicylate	157.5 ± 9.1

simulated patterns from their crystal structures, suggesting that each sample would contain a single crystalline phase with a fairly high purity. Moreover, these patterns are distinct from with the simulated patterns of MET-HCl forms A and B (Figures 1 and S1). Specifically, the diffractograms of CSL 2 and CSL S1−4 show characteristic peaks within the 15.0−17.0° region, but not for MET-HCl form A. The diffraction peaks within 12.0−13.0° from CSL 1 and 2 samples are also missing in MET-HCl form B. For CSL 3 and 4, and CSL S5, there exist peaks within the 5.0−11.0° region that are neither observed in the diffractogram of MET-HCl form A nor form B. Hence, the PXRD results strongly indicate that the salt preparation process yields crystalline phases other than the two known forms of MET-HCl.

3.1.2. FT-IR Spectroscopy. The FT-IR spectra of samples CSL 1 and 2 and CSL S1−5 are characterized by a weaker absorption in the region 1680−1720 cm^{-1} but a more intense peak in the region 1550−1650 cm^{-1} (Figures 2 and S2). Noting that the carbonyl stretch of carboxylic acid appears as a band in the former region and the asymmetric C−O stretch of carboxylate accounts for an absorption peak in the latter, this spectral characteristic could therefore indicate the formation of a carboxylate salt. Seemingly, the spectra of CSL 3 and 4 also share the same features, but certain subtle differences would require further attention. The strong absorption in the region 1550−1650 cm^{-1} shows an obvious blue shift, particularly for CSL 4. Meanwhile, no peak near 1400 cm^{-1} is observed for CSL 3, suggesting that the symmetric C−O stretch of carboxylate may be missing.[39,40] More importantly, the distinct peak in the region 1700−1750 cm^{-1}, which corresponds to the carbonyl stretch of ester for CSL S5, is absent for both CSL 3 and 4. Hence, the chemical compositions of CSL 3 and 4 may differ from that of CSL S5, and their polymorphic relationship with CSL S5 could possibly be ruled out.

3.1.3. SXRD. SXRD confirms that proton transfer occurred between metformin and organic acid. All CSL 2 and CSL S1−S5 comprise MET carboxylate salts and crystallize in a monoclinic space group $P2_1/n$ (or equivalence) except for CSL 1, which crystallize in a triclinic space group $P\bar{1}$ (Tables 1 and S1). MET formed 1:1 salt with formic acid (CSL S1), acetic acid (CSL S2), malonic acid (CSL S3), succinic acid, and acetylsalicylic acid (CSL S5). Meanwhile, MET formed a 2:1 salt with succinic acid (CSL S4), a 1:1 salt dihydrate with fumaric acid (CSL 1) and a 1:1 salt monohydrate with cinnamic acid (CSL 2). It is noteworthy that despite being a dicarboxylic acid originally, malonate tends to remain stable as a monoanion via an intramolecular hydrogen bond. A recently reported 1:1 3-(aminocarbonyl) pyridinium malonate salt exemplifies this phenomenon.[41] Interestingly, although fumaric acid exhibits the properties of a dicarboxylic acid, the two carboxylic acids in fumaric acid equivalently interact with the same MET molecule, thus finally forming a 1:1 salt. In addition, The C═O and C−O bond lengths of fumaric acid are 1.224 and 1.293 Å, and that of cinnamic acid are 1.259 and 1.279 Å, whereas the C═O and C−O bond lengths of carboxylic acids in CSL 1 and CSL 2 were 1.242 and 1.262 Å and 1.245 and 1.258 Å. This implies that even though carboxylic acids tend to be asymmetric, it is also possible to tell that the two form a salt based on the C−O bond distance.[42−44]

Within these seven MET carboxylate salts (CSL 1 and 2, and CSL S1−S5), the guanidine of MET connects with the carboxylate via a typical $R_2^2(8)$ cyclic hydrogen bond motif (Figures 3 and S3). This motif further dimerizes into a $R_4^4(16)$ cyclic motif, except for the fumarate dihydrate (CSL 1), the cinnamate monohydrate (CSL 2) and malonate (CSL S3). The presence of a water molecule also disrupts the dimerization of the guanidine-carboxylate motif in CSL 1 and 2. Due to an intramolecular hydrogen bond, the malonate in CSL S3 forms a substantial $R_4^4(24)$ motif instead. Apart from

https://doi.org/10.1021/acsomega.3c06721
ACS Omega 2023, 8, 48028−48041

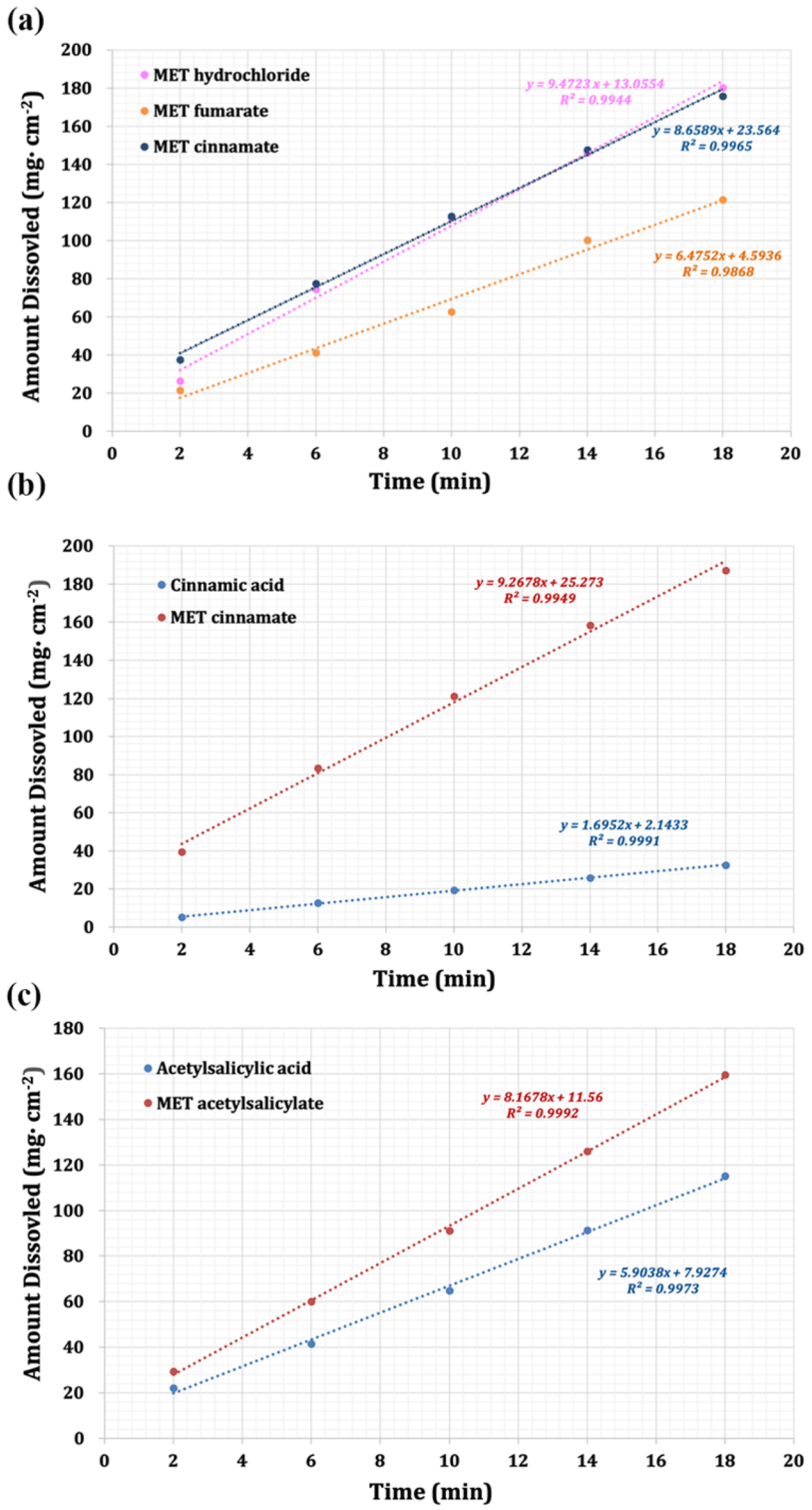

Figure 4. IDR test results of MET carboxylate salts in pH 6.8 phosphate buffer. Measured ingredients: (a) metformin, (b) cinnamic acid, and (c) acetylsalicylic acid.

these heterosynthons, guanidine with excess hydrogen bond capacity furthers a $R_2^2(8)$ homosynthon in all these salts except for CSL 1 and CSL S5 where a 1-D hydrogen bond chain is formed with the salicylate.

SXRD also confirms that, under a different experimental condition, MET has undergone chemical reaction and leads to crystals of two new substances, namely, CSL 3 and CSL 4, respectively (Table 1). CSL 3, a hemihydrate of a dihydro-1,3,5-triazine, crystallizes in the relatively rare tetragonal space group $P\bar{4}n2$. Due to proton disorder, the new derivative may exist in two tautomeric forms: N^4,N^4,6,6-tetramethyl-1,6-dihydro-1,3,5-triazine-2,4-diamine (tautomer 1) and N^2,N^2-6,6-tetramethyl-3,6-dihydro-1,3,5-triazine-2,4-diamine (tautomer 2). CSL 4, a 1:1 2-amino-4-(dimethylamino)-6-methyl-1,3,5-triazin-1-ium salicylate salt, crystallizes in the monoclinic space group $P2_1/n$. Regarding the hydrogen bond patterns,

https://doi.org/10.1021/acsomega.3c06721
ACS Omega 2023, 8, 48028−48041

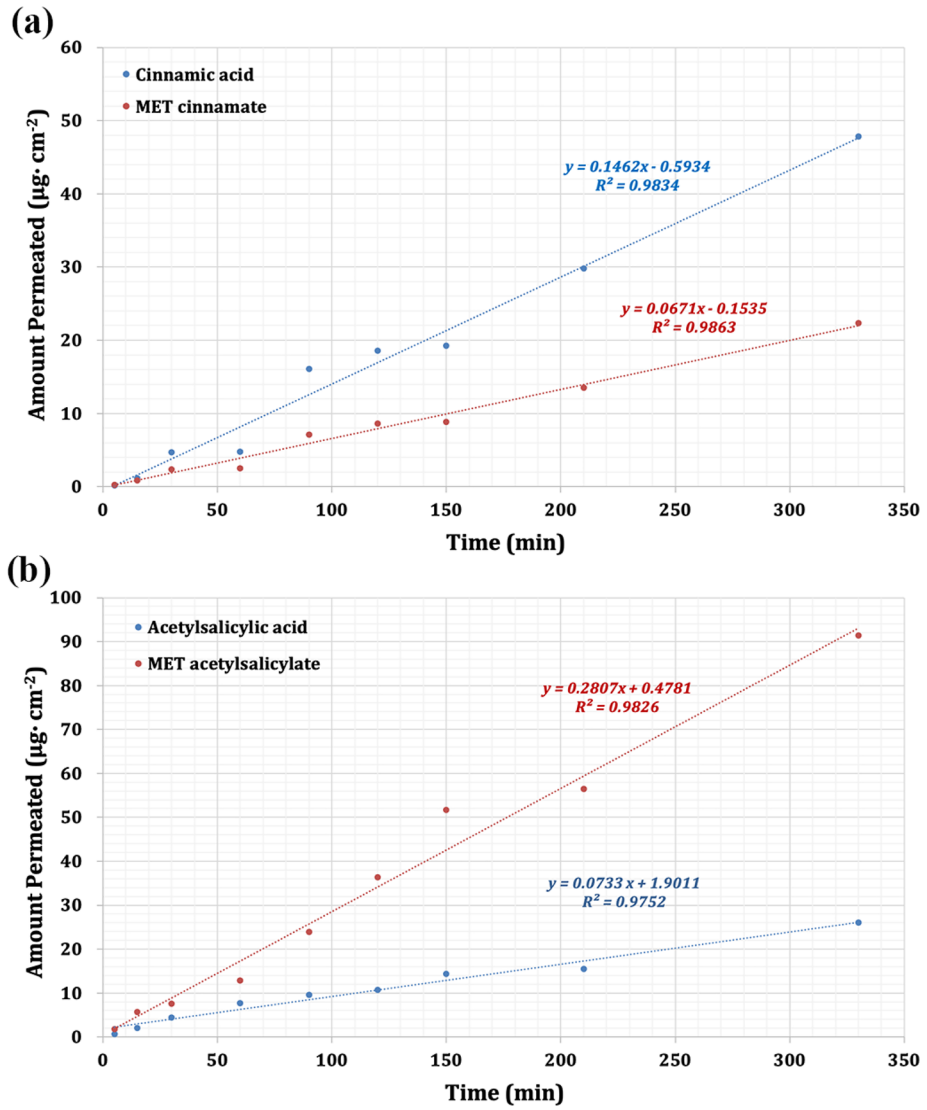

Figure 5. Cumulative amount of (a) cinnamic acid and (b) acetylsalicylic acid permeated vs time plot.

the triazine molecules in CSL 3 form a unique tetrameric $R_4^4(16)$ cyclic motif, and half water connects two triazines with a discrete $D_2^2(5)$ linkage. For CSL 4, the amino-triazinium pairs up with carboxylate via a $R_2^2(8)$ cyclic motif, which also results in a larger $R_4^4(16)$ cyclic motif after dimerization (Figure 3). The hydrogen bond parameters of all crystals are listed in Table 2.

3.2. Equilibrium Solubility Test and IDR Measurement. After determining the crystal structures and the chemical compositions, MET carboxylate salts CSL 1 and 2 and CSL S1−5 were subject to equilibrium solubility and IDR tests in pH 6.8 phosphate buffer. The results of the equilibrium solubility are shown in Table 3. Although the equilibrium solubility of all MET slats did not exceed the equilibrium solubility of MET hydrochloride, they were all easily soluble (>0.1 g/mL). The result makes the dissolution rate of these salts and the corresponding ligands becoming the focus of attention. In IDR test, all seven salts show varying aqueous solubilities (Figures 4 and S4). Since metformin hydrochloride began to show disruption of the dissolution surface at approximately 18 min into the IDR experiment, only the first 18 min of sampling time points were considered for the experiment. For MET, metformin hydrochloride has the highest dissolution rate (1.0), and the relative dissolution rate of other organic acids is in the following order: CSL 2 (MET cinnamate, 0.91) > CSL S1 (MET formate, 0.91) > CSL S2 (MET acetate, 0.83) > CSL S4 (MET succinate, 0.80) > CSL S3 (MET malonate, 0.76) > CSL 1 (MET fumarate, 0.68) > CSL S5 (MET acetylsalicylate, 0.52). Among them, MET cinnamate showed a better dissolution rate, which was comparable to MET hydrochloride, and MET acetylsalicylate's dissolution rate was relatively poor, about half of MET hydrochloride. At the same time, the dissolution rate of the two active ligands was also investigated. Compared with the cinnamic acid and acetylsalicylic acid, the dissolution rate after salt formation increased by 5.5 times and 1.4 times, respectively. This is beneficial for improving the bioavailability of them. First, this could be due to the fact that metformin forms salts with organic acids, which have better solubility in the ionic state compared to neutral compounds. In addition, when the salt is dissolved in the solvent, the MET provides an alkaline microenvironment that is more favorable for the dissolution of the acid, thus increasing the rate of dissolution of the

https://doi.org/10.1021/acsomega.3c06721
ACS Omega 2023, 8, 48028−48041

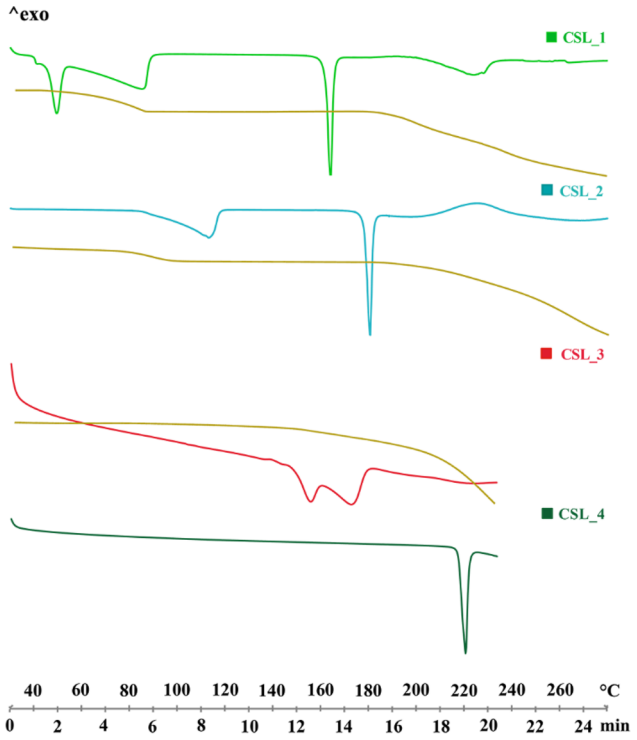

Figure 6. DSC curves of CSL 1−4 with additional TGA plots (colored dark yellow) for the three hydrates of CSL 1−3.

CCF.[45] Finally, due to their rapid dissolution rates in pH 6.8 phosphate buffer, a 90% isopropanol-water solvent mixture was chosen as an alternative dissolution medium, and corresponding results are shown in Supporting Information (Figure S5).

3.3. Permeability Analysis. Metformin is a BCS Class III compound; therefore, whether the formation of organic acid salts can improve the permeability of MET is an aspect worthy of attention. In this paper, the permeability of MET was preliminarily evaluated by the Franz diffusion cell method. Unfortunately, the results showed that the formation of organic acids did not improve the permeability of MET. However, studies have shown that metformin salts can increase the permeability of the corresponding ligand. Therefore, the permeability of the active ligands of CSL 2 and CSL S5, namely, cinnamic acid and acetylsalicylic acid, was investigated. The results showed that the permeability of cinnamic acid was decreased, while that of acetylsalicylic acid was increased to a certain extent (Figure 5). This also reflects to a certain extent why cinnamate did not further improve the hypoglycemic effect. In addition, it also suggests that acetylsalicylate may be more antipyretic and analgesic than acetylsalicylic acid itself.

3.4. Thermal Analysis. The three hydrates CSL 1−3 show dual endothermic events upon heating, corresponding to dehydration and melting, respectively (Figure 6). For CSL 1, the dehydration process takes place at approximate 40−90 °C appearing as a double peak alongside a weight loss of 12.5%, consistent with the stoichiometry for a dihydrate of fumarate salt. For CSL 2, the first endothermic event at 112.6 °C takes place alongside a weight loss of 6.1%, consistent with the stoichiometry for a monohydrate of cinnamate salt. For CSL 3, the two overlapped endothermic peaks suggest the co-occurrence of both dehydrate and melting. A 4.7% weight loss across this temperature range matches the hemihydrate of this new triazine derivative. The remaining samples only show a single melting event, and the measured peak melting point of the MET carboxylate (excluding CSL 1 and 2) in ascending order is CSL S1 < CSL S5 < CSL S3 < CSL S2 < CSL S4 (Figures 6 and S6). Apparently, the MET carboxylate salts with faster dissolution rates (CSL S1 and CSL S5) have marginally lower melting points than those that dissolve more slowly.

3.5. Theoretical Calculation. *3.5.1. Packing Similarity MET Salts.* Melting temperature can be conceptually predicted from both the melting enthalpy and entropy. These physical quantities are related to the strength of intermolecular interactions and the internal symmetry of the molecule itself, respectively. In light of common H-bond motifs among the CSL structures, the possibility of isostructural packing and its potential influence on molecular interaction (and possibly dissolution rate) is therefore investigated. The packing similarity search includes the seven MET carboxylate salts (CSL 1−2 and CSL S1−5) and both MET-HCl (forms A and B). The resulting dendrogram shows that CSL S1, CSL S2, and CSL S4 are nearly isostructural to one another, whereas other structures have quite distinct packing (Figure 7). Formate (CSL S1) and acetate (CSL S2) appear interchangeable in the crystalline state without significant altering of the lattice parameters. Succinate (CSL S4) could be substituted into the space where two acetate ions have a head-on methyl group contact. Despite the monoanion form of malonate (CSL S3), the neutral electronegative carboxylic group may result in an unfavorable packing when substituted into the lattices of CSL S1 or S2, and therefore leads to an alternative packing. For cinnamate (CSL 2) and acetylsalicylate (CSL S5), both anions have distinct differences in shape and size when compared to small carboxylic acids, and dissimilar packings are expected. Nevertheless, isostructurality may only explain the slow dissolution rates of CSL S2 and CSL S4, but it

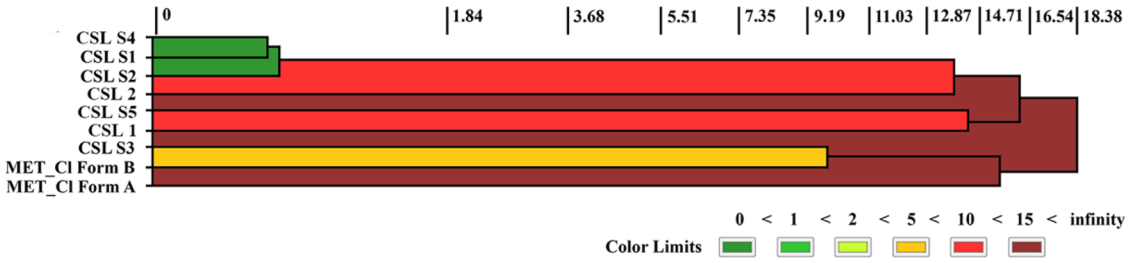

Figure 7. Packing similarity dendrogram of the MET salts. A calculated score closer to zero indicates a higher similarity between the crystals. Only MET molecules were considered.

https://doi.org/10.1021/acsomega.3c06721
ACS Omega 2023, 8, 48028−48041

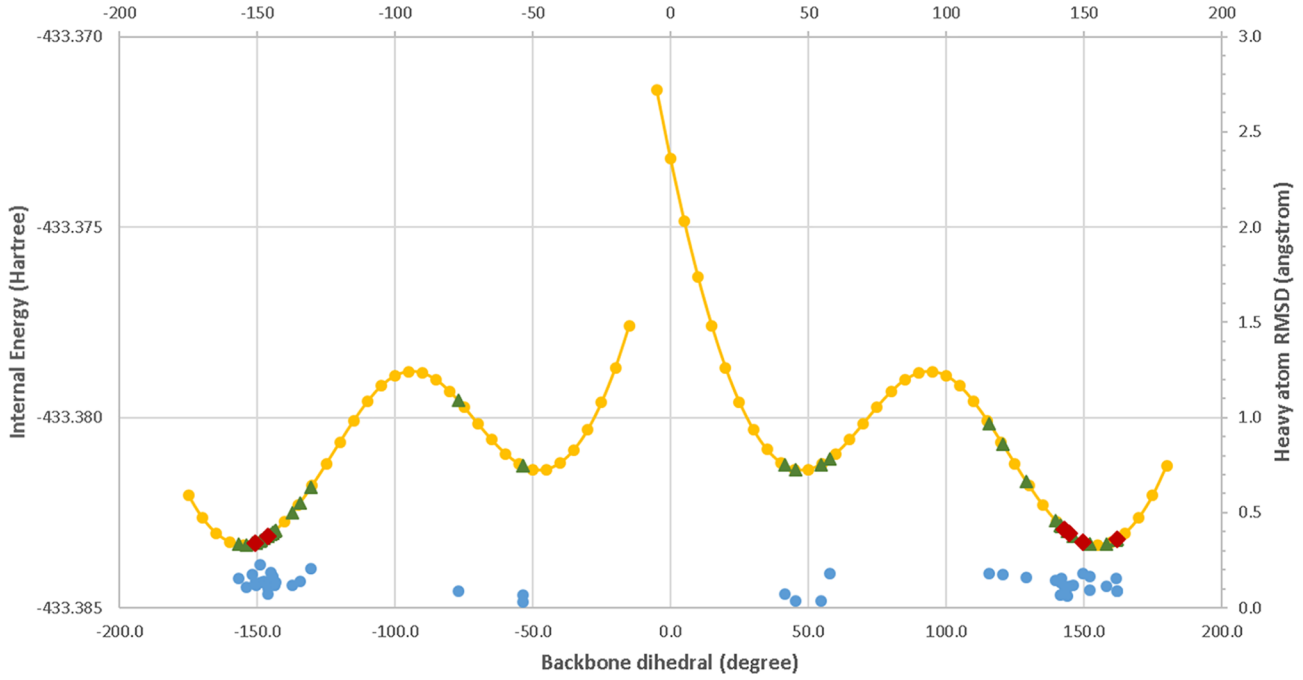

Figure 8. Potential energy surface of backbone dihedral angle of MET at B3LYP/6-311G** level (yellow), the optimized conformers from 27 salts in CSD (green) and six MET-organic salts (red), and the RMSDs of heavy atoms in MET after the gas phase optimizations (blue).

would be insufficient to address the faster dissolution rate of CSL S1. Meanwhile, dissimilar structures also show diverse dissolution behaviors, with CSL 2 and CSL S5 having rates superior to those of CSL 3.

3.5.2. Conformation Analysis of MET. The degree of isostructurality among the MET carboxylates does not fully account for the difference in their dissolution rates. Since such a search focuses primarily on the geometries of MET, conformation analysis from first-principles would help understanding the relative stability of the molecular cation. A rigid grid scan was performed upon its backbone dihedral angle, which characterizes the conformation of MET. The potential energy surface at B3LYP/6-311G** level shows four energy minima at +50, −50, +155, and −155° (Figure 8, yellow dots). According to the Boltzmann distribution at 300 K, the normalized probability of each minimum would be 5.5% (for ±50°) and 44.5% (for ±155°) respectively. In addition, 43 MET conformers extracted from 27 reported MET containing crystal structures (Figure 8, green triangles) and six MET carboxylates (Figure 8, red diamonds) show RMSDs of heavy atoms not more than 0.25 Å (Figure 8, blue dots), after all internal coordinates except for this backbone dihedral angle were optimized. The low RMSDs indicate that the MET conformers are still geometrically in good concordance after optimizations. Moreover, the majority of the conformers lie in the +155 or −155° energy minima, and only seven out of the 43 conformers locate in either the +50 or −50° minima. The former group has an occurrence ratio of 41.9%, whereas the latter is around 5−7%. This outcome suggests that the gas phase calculation is consistent with the prevalence of conformers observed in the lattices. Nevertheless, some MET conformers observed in crystal structures show much greater deviations from the above-mentioned energy minima. For example, the dihedral angle of MET in VOPLAO (−77.1°) and one of the MET conformers in YOKVUR (+115.7°) deviate from their nearest energy minima by more than 20° (Figure 8). Even the highly unstable form B of MET-HCl has a MET conformer 0.25 kcal/mol more stable than that of form A in the gas phase. Clearly, the packing effect in crystalline environments may have offered extra stability to the metastable conformations of MET in the gas phase.

3.6. Effect of MET-Drug Salts and Novel Derivatives on Glucose Metabolism and Cell Viability. Since the MET-cinnamate (CSL 2) and MET-acetylsalicylate (CSL S5) have shown advantageous dissolution rates in the test medium, their *in vitro* effects on glucose consumption and cellular viability were further investigated alongside their counterions (cinnamic acid and acetylsalicylic acid), salicylic acid, and the two triazine derivatives (CSL 3 and 4). Previous studies showed that detecting the glucose consumption in hepatic cells becomes a simple and sensitive cell-based methodology for hypoglycemic drug screening.[46] In the present study, 2 mM MET-HCl was confirmed to accelerate the glucose consumption in HepG2 cells (Figure 9a). At the same concentration, the two MET salts (CSL 2 and CSL S5), cinnamic acid, and acetylsalicylic acid could also significantly increase the glucose consumption. Interestingly, MET-acetylsalicylate (CSL S5) and CSL 3 have more profound effects on accelerating glucose consumption over MET-HCl at such a concentration. However, the other triazine derivate, CSL 4, and salicylic acid showed no significant effect on glucose consumption.

When regulating glucose metabolism, MET induces lactic acid production which results in lactic acidosis as a main side effect.[47,48] Thus, *in vitro* lactic acid release caused by these MET salts, triazine derivatives and related compounds was studied (Figure 9b). Only MET-HCl and acetylsalicylate, CSL 3, and acetylsalicylic acid can promote the production of lactic acid significantly, while the cinnamate salt and other compounds have no significant effect on the lactic acid levels. Additionally, the effects of the salts and compounds on cell

https://doi.org/10.1021/acsomega.3c06721
ACS Omega 2023, 8, 48028−48041

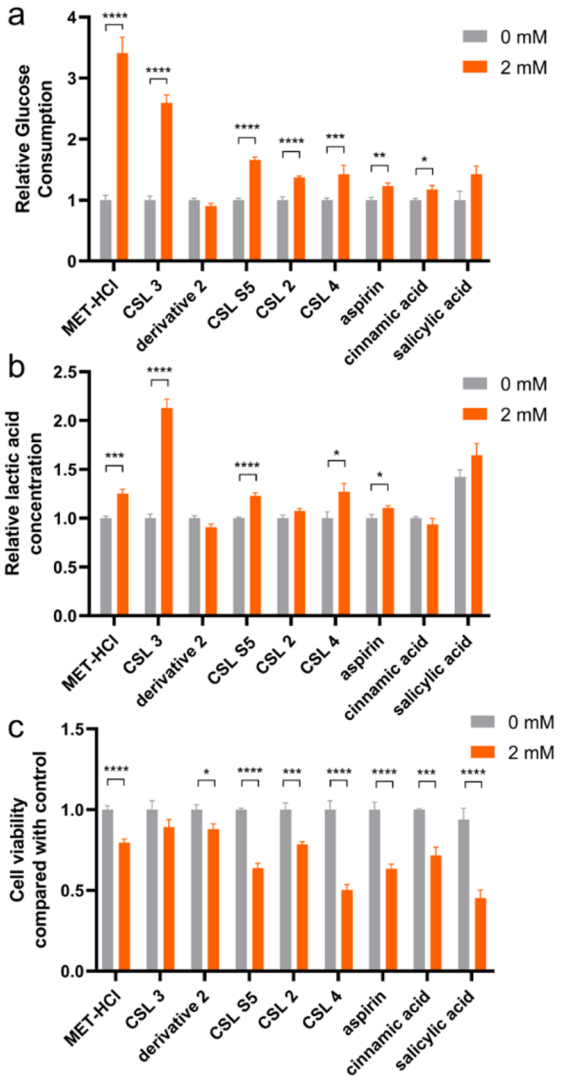

Figure 9. Effects of CSL 2−4 and S5, cinnamic acid, acetylsalicylic acid, and salicylic acid on glucose consumption, lactic acid release, and cell viability in hepatic HepG2 cells in vitro.

viability were also detected (Figure 9c). All, except the monomer of CSL 3, significantly reduce the viability of HepG2 cells.

The studies described above reveal that triazine CSL3 has relatively better activity in the regulation of glucose metabolism among the tested MET salts and compounds. To verify the efficacy of CSL 3, the concentration for investigation was extended to 5, 10, and 20 mM, respectively. As shown in Figure 10a, both MET-HCl and CSL 3 accelerate the glucose consumption in HepG2 cells in a concentration-dependent manner. They were also found to promote the production of lactic acid with increasing dose, but CSL 3 induces lactic acid production to a lesser extent at lower concentrations (2 and 5 mM), when compared with MET-HCl (Figure 10b). In addition, both MET-HCl and CSL 3 also reduce the viability of HepG2 cells in a concentration-dependent manner, but their cytotoxicity becomes significant beyond a concentration of 2 mM (Figure 10c).

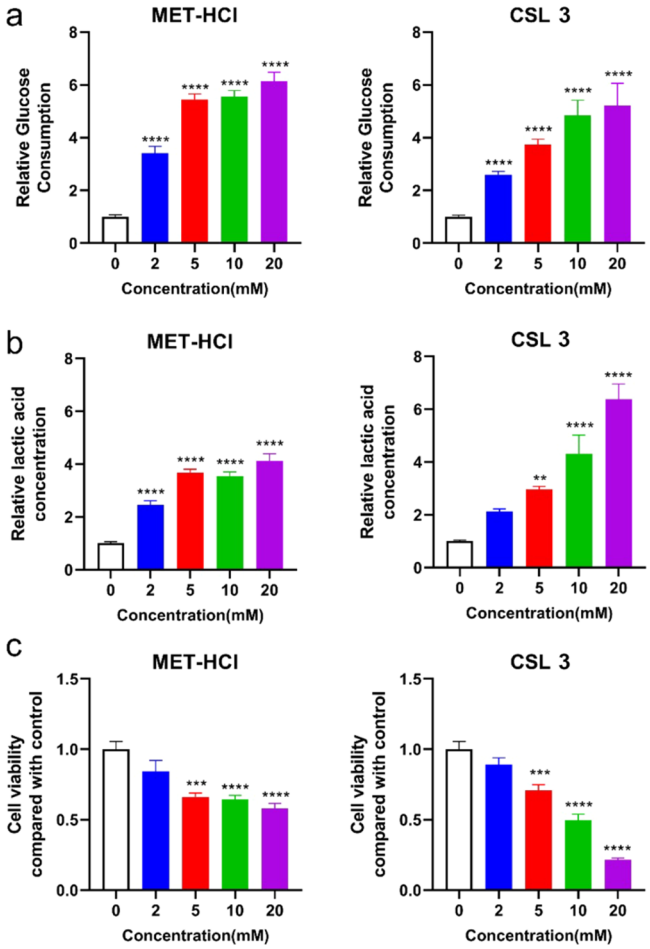

Figure 10. Effects of MET-HCl and CSL 3 at increased concentrations on glucose consumption, lactic acid release, and cell viability in hepatic HepG2 cells in vitro.

4. CONCLUSIONS

Five metformin carboxylate salts and two salt hydrates were successfully prepared. To the best of our knowledge, two crystal forms of MET-fumarate dihydrate and MET-cinnamate monohydrate were reported for the first time. The pharmaceutical properties of these crystal forms, notably the intrinsic dissolution rate, were systematically investigated. In pH 6.8 phosphate buffer, all these salts and salt hydrates show slower dissolution rates than metformin hydrochloride, which are consistent with the published results for the previously reported salts. Interestingly, the dissolution rates of the counterions cinnamate and acetylsalicylate were improved upon salt formation with metformin.

The calculated ionization energy seems to have a weak correlation to the measured dissolution rates in the 90% isopropanol−water solvent mixture. The enthalpy of dissolution, which takes into account the solvation enthalpy, shows a stronger correlation to dissolution rates, implying that the solvation of ionic molecular species contributes significantly to the dissolution process of these crystal forms (discussed in Supporting Information). With apparently better dissolution rates than the hydrochloride in this kind of dissolution medium, the cinnamate hydrate and acetylsalicylate at 2 mM also significantly increase glucose consumption in HepG2 cells against control. However, only the latter shows a higher relative glucose consumption over

https://doi.org/10.1021/acsomega.3c06721
ACS Omega 2023, 8, 48028−48041

hydrochloride salt, probably due to an additive effect from the acetylsalicylate. In contrast, cinnamate hardly inflicts a similar effect to the salt complex.

Surprisingly, two triazine derivatives were discovered during the preparation of metformin acetylsalicylate, indicating that the chemical reaction could not be ruled out during salt preparation. The reaction mechanisms suggest that the solvent of choice and the chemical stability of the involved molecules may be attributed to the emergence of these unexpected chemical species. FTIR sheds light on the chemical integrity in samples and complements other spectroscopic techniques in any potentially novel crystal forms. Nevertheless, the triazine derivative in CSL 3 (as a hemihydrate) demonstrates an excellent in vitro profile as an antihyperglycemic agent: At a low dose with tolerable cytotoxicity, its relative glucose consumption is nearly twice that of the hydrochloride salt. Further molecular optimizations would be required for lowering its induction effect on lactic acid production before obtaining a promising lead compound against diabetes mellitus. It is noteworthy to mention that the other triazine derivative in CSL 4 is structurally similar to that in CSL 3. Strikingly, with only one methyl group missing, its *in vitro* bioactivities are literally abolished. The underlying reason for this phenomenon would be highly valuable for ligand-based drug design, in order to develop a novel triazine antihyperglycemic agent.

■ ASSOCIATED CONTENT

Supporting Information

The Supporting Information is available free of charge at https://pubs.acs.org/doi/10.1021/acsomega.3c06721.

Table S1−S2 and Figure S1−S6 specific information can be found in the support information (PDF)

■ AUTHOR INFORMATION

Corresponding Authors

Dezhi Yang − *Beijing City Key Laboratory of Polymorphic Drugs, Center of Pharmaceutical Polymorphs, Institute of Materia Medica, Chinese Academy of Medical Sciences and Peking Union Medical College, Beijing 100050, P.R. China*; orcid.org/0000-0002-3159-4126; Email: ydz@imm.ac.cn

Li Zhang − *Beijing City Key Laboratory of Polymorphic Drugs, Center of Pharmaceutical Polymorphs, Institute of Materia Medica, Chinese Academy of Medical Sciences and Peking Union Medical College, Beijing 100050, P.R. China*; orcid.org/0000-0003-3115-8196; Email: zhangl@imm.ac.cn

Yang Lu − *Beijing City Key Laboratory of Polymorphic Drugs, Center of Pharmaceutical Polymorphs, Institute of Materia Medica, Chinese Academy of Medical Sciences and Peking Union Medical College, Beijing 100050, P.R. China*; orcid.org/0000-0002-2274-5703; Email: luy@imm.ac.cn

H. C. Stephen Chan − *Shenzhen Zhongke Cedar Tree Trading Company, Shenzhen, Guangdong 518017, P.R. China*; Email: actmol.info@gmail.com

Authors

Qi An − *Beijing City Key Laboratory of Polymorphic Drugs, Center of Pharmaceutical Polymorphs, Institute of Materia Medica, Chinese Academy of Medical Sciences and Peking Union Medical College, Beijing 100050, P.R. China*

Na Li − *Beijing City Key Laboratory of Drug Target and Screening Research, National Center for Pharmaceutical Screening, Institute of Materia Medica, Chinese Academy of Medical Sciences and Peking Union Medical College, Beijing 100050, P.R. China*

Zhehui Zhao − *State Key Laboratory of Bioactive Substance and Function of Natural Medicines, Beijing Key Laboratory of Active Substances Discovery and Drugability Evaluation, Institute of Materia Medica, Chinese Academy of Medical Sciences and Peking Union Medical College, Beijing 100050, P.R. China*

Nuoqi Wang − *Beijing City Key Laboratory of Drug Target and Screening Research, National Center for Pharmaceutical Screening, Institute of Materia Medica, Chinese Academy of Medical Sciences and Peking Union Medical College, Beijing 100050, P.R. China*

Xueying Wang − *BayRay Innovation Center, Shenzhen Bay Laboratory, Shenzhen, Guangdong 518000, P.R. China*

Xiuying Yang − *Beijing City Key Laboratory of Drug Target and Screening Research, National Center for Pharmaceutical Screening, Institute of Materia Medica, Chinese Academy of Medical Sciences and Peking Union Medical College, Beijing 100050, P.R. China*

Guanhua Du − *Beijing City Key Laboratory of Drug Target and Screening Research, National Center for Pharmaceutical Screening, Institute of Materia Medica, Chinese Academy of Medical Sciences and Peking Union Medical College, Beijing 100050, P.R. China*

Complete contact information is available at: https://pubs.acs.org/10.1021/acsomega.3c06721

Author Contributions

#Qi An and Na Li contributed equally to this work. Qi An: Formal analysis, Writing - original draft. Na Li: Formal analysis, Writing - original draft. Zhehui Zhao: Formal analysis. Nuoqi Wang: Formal analysis. Xueying Wang: Formal analysis. Xiuying Yang: Formal analysis. Dezhi Yang: Investigation, Review & Editing, Supervision, Funding acquisition. Li Zhang: Review & Editing, Supervision. Yang Lu: Review & Editing, Supervision, Funding acquisition. Guanhua Du: Review & Editing, Supervision. HC Stephen Chan: Review & Editing, Supervision.

Notes

The authors declare no competing financial interest.

■ ACKNOWLEDGMENTS

The authors acknowledge the National Natural Science Foundation of China (Grant No. 22278443), CAMS Innovation Fund for Medical Sciences (Grant No. 2022-I2M-1-015), the Chinese Pharmacopoeia Commission Drug Standard Promoting Fund (Grant No. 2022Y14), and research grant from Guangdong Province (Grant No. 2022A1515011792) for financing this work. Authors would like to thank Shenzhen Institutes of Advacned Technology for supporting computational resources.

■ REFERENCES

(1) Foretz, M.; Guigas, B.; Viollet, B. Understanding the Glucoregulatory Mechanisms of Metformin in Type 2 Diabetes Mellitus. *Nat. Rev. Endocrinol.* **2019**, *15*, 569−589.

(2) Kulkarni, A. S.; Gubbi, S.; Barzilai, N. Benefits of Metformin in Attenuating the Hallmarks of Aging. *Cell Metab.* **2020**, *32*, 15−30.
(3) Wang, Y.; An, H.; Liu, T.; Qin, C.; Sesaki, H.; Guo, S.; Radovick, S.; Hussain, M.; Maheshwari, A.; Wondisford, F. E.; O'Rourke, B.; He, L. Metformin Improves Mitochondrial Respiratory Activity through Activation of AMPK. *Cell Rep.* **2019**, *29*, 1511−1523.
(4) Plata-Vargas, E.; De la Cruz-Hernández, C.; Dorazco-González, A.; Fuentes-Noriega, I.; Morales-Morales, D.; Germán-Acacio, J. M. Synthesis of Metforminium Succinate by Melting. Crystal Structure, Thermal, Spectroscopic and Dissolution Properties. *J. Mex. Chem. Soc.* **2017**, *61*, 197−204.
(5) Lara Ochoa, J. M. F. Metformin-based ionic co-crystal. WO2012148252A2, 2012.
(6) Huttunen, K. M.; Mannila, A.; Laine, K.; Kemppainen, E.; Leppanen, J.; Vepsalainen, J.; Jarvinen, T.; Rautio, J. The First Bioreversible Prodrug of Metformin with Improved Lipophilicity and Enhanced Intestinal Absorption. *J. Med. Chem.* **2009**, *52*, 4142−4148.
(7) Diniz, L. F.; Carvalho, P. S.; Gonçalves, J. E.; Diniz, R.; Fernandes, C. Solid-state landscape and biopharmaceutical implications of novel metformin-based salts. *New J. Chem.* **2022**, *46*, 13725−13737.
(8) McCreight, L. J.; Bailey, C. J.; Pearson, E. R. Metformin and the gastrointestinal tract. *Diabetologia* **2016**, *59*, 426−435.
(9) Saines, P. CSD Communication (Private Communication), 2022, CCDC 2157999.
(10) Hassan, A. R.; El-Kousy, S. M.; El-Toumy, S. A.; Frydenvang, K.; Tung, T. T.; Olsen, J.; Nielsen, J.; Christensen, S. B. Metformin, an Anthropogenic Contaminant of Seidlitzia rosmarinus Collected in a Desert Region near the Gulf of Aqaba, Sinai Peninsula. *J. Nat. Prod.* **2017**, *80*, 2830.
(11) Diniz, L. F.; Carvalho, P. S.; Gonçalves, J. E.; Diniz, R.; Fernandes, C. Solid-state landscape and biopharmaceutical implications of novel metformin-based salts. *New J. Chem.* **2022**, *46*, 13725−13737.
(12) Zhou, W. X.; Zhao, H. W.; Chen, H. H.; Zhang, Z. Y.; Chen, D. Y. Characterization of drug−drug salt forms of metformin and aspirin with improved physicochemical properties. *CrystEngComm* **2019**, *21*, 3770−3773.
(13) Plata-Vargas, E.; De la Cruz-Hernandez, C.; Dorazco-Gonzalez, A.; Fuentes-Noriega, I.; Morales-Morales, D.; German-Acacio, J. M. *Mex.Chem. Soc.* **2017**, *61*, 197−204.
(14) Adisakwattana, S. Cinnamic Acid and Its Derivatives: Mechanisms for Prevention and Management of Diabetes and Its Complications. *Nutrients* **2017**, *9*, 163.
(15) Hafizur, R. M.; Hameed, A.; Shukrana, M.; Raza, S. A.; Chishti, S.; Kabir, N.; Siddiqui, R. A. Cinnamic Acid Exerts Anti-Diabetic Activity by Improving Glucose Tolerance in Vivo and by Stimulating Insulin Secretion in Vitro. *Phytomedicine* **2015**, *22*, 297−300.
(16) ICH. Guideline ICH Harmonised Tripartite. *Stability Testing of New Drug Substances and Products Q1A (R2)*; 2003; Vol. *4*, pp 1−24.
(17) Feng, W. Q.; Wang, L. Y.; Gao, J.; Zhao, M. Y.; Li, Y. T.; Wu, Z. Y.; Yan, C. W. Solid state and solubility study of a potential anticancer drug-drug molecular salt of diclofenac and metformin. *J. Mol. Struct.* **2021**, *1234*, 130166.
(18) Macrae, C. F.; Edgington, P. R.; McCabe, P.; Pidcock, E.; Shields, G. P.; Taylor, R.; Towler, M.; Van De Streek, J. Mercury: Visualization and Analysis of Crystal Structures. *J. Appl. Crystallogr.* **2006**, *39*, 453−457.
(19) Dolomanov, O. V.; Bourhis, L. J.; Gildea, R. J.; Howard, J. A. K.; Puschmann, H. OLEX2: A Complete Structure Solution, Refinement and Analysis Program. *J. Appl. Crystallogr.* **2009**, *42*, 339−341.
(20) Burla, M. C.; Caliandro, R.; Camalli, M.; Carrozzini, B.; Cascarano, G. L.; De Caro, L.; Giacovazzo, C.; Polidori, G.; Siliqi, D.; Spagna, R. IL MILIONE: A Suite of Computer Programs for Crystal Structure Solution of Proteins. *J. Appl. Crystallogr.* **2007**, *40*, 609−613.
(21) Sheldrick, G. M. Crystal structure refinement with SHELXL. *Acta Cryst. C Struct. Chem.* **2015**, *71*, 3−8.
(22) Müller, P.; Herbst-Irmer, R.; Spek, A. L.; Schneider, T. R.; Sawaya, M. R. *Crystal Structure Refinement: A Crystallographer's Guide to SHELXL* **2010**, 1−232.
(23) Chinese Pharmacopoeia Commission. *Chinese Pharmacopoeia*; China Medical Science and Technology Press, 2020.
(24) Rohlíček, J.; Skořepová, E.; Babor, M.; Čejka, J. CrystalCMP: An Easy-to-Use Tool for Fast Comparison of Molecular Packing. *J. Appl. Crystallogr.* **2016**, *49*, 2172−2183.
(25) Lu, T. *Molclus program*, version 1.9.3; http://www.keinsci.com/research/molclus.html (accessed 7/5/2020).
(26) Frisch, M.; Trucks, G.; Schlegel, H.; Scuseria, G.; Robb, M.; Cheeseman, J.; Scalmani, G.; Barone, V.; Petersson, G.; Nakatsuji, H. *Gaussian 16*, revision A.03; Gaussian, Inc.: Wallingford, CT, 2016.
(27) Giannozzi, P.; Baroni, S.; Bonini, N.; Calandra, M.; Car, R.; Cavazzoni, C.; Ceresoli, D.; Chiarotti, G. L.; Cococcioni, M.; Dabo, I.; Dal Corso, A.; et al. QUANTUM ESPRESSO: a modular and open-source software project for quantum simulations of materials. *J. Phys.: Condens. Matter* **2009**, *21*, 395502.
(28) Giannozzi, P; Andreussi, O; Brumme, T; Bunau, O; Buongiorno Nardelli, M; Calandra, M; Car, R; Cavazzoni, C; Ceresoli, D; Cococcioni, M; Colonna, N; Carnimeo, I; Dal Corso, A; de Gironcoli, S; Delugas, P; DiStasio, R A; Ferretti, A; Floris, A; Fratesi, G; Fugallo, G; Gebauer, R; Gerstmann, U; Giustino, F; Gorni, T; Jia, J; Kawamura, M; Ko, H-Y; Kokalj, A; Kucukbenli, E; Lazzeri, M; Marsili, M; Marzari, N; Mauri, F; Nguyen, N L; Nguyen, H-V; Otero-de-la-Roza, A; Paulatto, L; Ponce, S; Rocca, D; Sabatini, R; Santra, B; Schlipf, M; Seitsonen, A P; Smogunov, A; Timrov, I; Thonhauser, T; Umari, P; Vast, N; Wu, X; Baroni, S Advanced capabilities for materials modelling with Quantum ESPRESSO. *J. Phys.: Condens. Matter.* **2017**, *29*, 465901.
(29) Perdew, J. P.; Burke, K.; Ernzerhof, M. Generalized Gradient Approximation Made Simple. *Phys. Rev. Lett.* **1996**, *77*, 3865−3868.
(30) Dal Corso, A. Pseudopotentials Periodic Table: From H to Pu. *Comput. Mater. Sci.* **2014**, *95*, 337−350.
(31) Otero-De-La-Roza, A.; Johnson, E. R. Van Der Waals Interactions in Solids Using the Exchange-Hole Dipole Moment Model. *J. Chem. Phys.* **2012**, *136*, No. 174109.
(32) Martyna, G. J.; Tuckerman, M. E. A Reciprocal Space Based Method for Treating Long Range Interactions in Ab Initio and Force-Field-Based Calculations in Clusters. *J. Chem. Phys.* **1999**, *110*, 2810−2821.
(33) Barone, V.; Cossi, M. Conductor Solvent Model. *J. Phys. Chem. A* **1998**, *102*, 1995−2001.
(34) Neese, F. The ORCA Program System. *Wiley Interdiscip. Rev.: Comput. Mol. Sci.* **2012**, *2*, 73−78.
(35) Neese, F. Software update: the ORCA program system, version 4.0. *Wiley Interdiscip. Rev.: Comput. Mol. Sci.* **2018**, *8*, e1327.
(36) Marenich, A. V.; Cramer, C. J.; Truhlar, D. G. Universal Solvation Model Based on Solute Electron Density and on a Continuum Model of the Solvent Defined by the Bulk Dielectric Constant and Atomic Surface Tensions. *J. Phys. Chem. B* **2009**, *113*, 6378−6396.
(37) Shi, L. L.; Jia, W. H.; Zhang, L.; Xu, C. Y.; Chen, X.; Yin, L.; Wang, N. Q.; Fang, L. H.; Qiang, G. F.; Yang, X. Y.; Du, G. H. Glucose Consumption Assay Discovers Coptisine with Beneficial Effect on Diabetic Mice. *Eur. J. Pharmacol.* **2019**, *859*, 172523.
(38) Zhang, L.; Hu, J. J.; Du, G. H. Establishment of a Cell-Based Assay to Screen Insulin-like Hypoglycemic Drugs. *Drug Discovery Ther.* **2008**, *2*, 229−233.
(39) Binev, I. G.; Stamboliyska, B. A.; Binev, Y. I. The Infrared Spectra and Structure of Acetylsalicylic Acid (Aspirin) and Its Oxyanion: An Ab Initio Force Field Treatment. *J. Mol. Struct.* **1996**, *378*, 189−197.

https://doi.org/10.1021/acsomega.3c06721
ACS Omega 2023, 8, 48028−48041

(40) Cerreia Vioglio, P.; Chierotti, M. R.; Gobetto, R. Pharmaceutical aspects of salt and salt forms of APIs and characterization challenges. *Adv. Drug Deliver. Rev.* **2017**, *117*, 86−110.
(41) Stainton, P.; Nauha, E.; Grecu, T.; McCabe, J. F.; Munshi, T.; Scowen, I.; Chan, H. C. S.; Nilsson, S.; Blagden, N. Chameleon Behavior of a New Salt of 3-(Aminocarbonyl) Pyridinium Malonate and Implications for Polymorphism on the Salt/Cocrystal Continuum. *Cryst. Growth Des.* **2022**, *22*, 1665−1679.
(42) Sánchez-Lombardo, I.; Sánchez-Lara, E.; Pérez-Benítez, A.; Mendoza, Á.; Bernès, S.; González-Vergara, E. Synthesis of Metforminium (2 +) Decavanadates − Crystal Structures and Solid-State Characterization. *Eur. J. Inorg. Chem.* **2014**, *2014*, 4581−4588.
(43) Yu, H.; Zhang, L.; Liu, M.; Yang, D.; He, G.; Zhang, B.; Gong, N.; et al. Enhancing Solubility and Dissolution Rate of Antifungal Drug Ketoconazole through Crystal Engineering. *Pharmaceuticals* **2023**, *16*, 1349.
(44) Basavoju, S.; Boström, D.; Velaga, S. P. Pharmaceutical cocrystal and salts of norfloxacin. *Cryst. Growth Des.* **2006**, *6*, 2699−2708.
(45) Babu, N. J.; Nangia, A. Solubility Advantage of Amorphous Drugs and Pharmaceutical Cocrystals. *Cryst. Growth Des.* **2011**, *11*, 2662−2679.
(46) Okajima, T.; Nakamura, K.; Zhang, H.; Ling, N.; Taabe, T.; Yasuda, T.; Rosenfeld, R. G. Sensitive colorimetric bioassays for insulin-like growth factor (IGF) stimulation of cell proliferation and glucose consumption: use in studies of IGF analogs. *Endocrinology* **1992**, *130*, 2201−212.
(47) Rhee, C. M.; Kalantar-Zadeh, K. Diabetes Mellitus: Complex Interplay between Metformin, AKI and Lactic Acidosis. *Nat. Rev. Nephrol.* **2017**, *13*, 521−522.
(48) Lazarus, B.; Wu, A.; Shin, J. I.; Sang, Y.; Alexander, G. C.; Secora, A.; Inker, L. A.; Coresh, J.; Chang, A. R.; Grams, M. E. Association of Metformin Use with Risk of Lactic Acidosis across the Range of Kidney Function: A Community-Based Cohort Study. *JAMA Int. Med.* **2018**, *178*, 903−910.

https://doi.org/10.1021/acsomega.3c06721
ACS Omega 2023, 8, 48028−48041